

Length-based adequacy thresholds for submandibular gland core needle biopsy in suspected Sjögren's disease: two-phase study

C.-F. Cheng^{1,2}, T.-C. Chen³, M.-S. Hsieh⁴, T.-Y. Lan⁵, C.-Y. Huang⁴, J.-H. Kao⁶, Y.-H. Lin⁷, C. Wang⁸, H.-N. Huang⁹, L.-W. Lin¹⁰, Y.-J. Chiang¹¹, M.-F. Cheng¹², H.-S. Chu^{2,13}, Y.-M. Huang^{2,14}, C.-H. Lu^{1,2}, K.-J. Li¹, C.-Y. Shen¹, S.-C. Hsieh¹

¹Department of Internal Medicine, National Taiwan University Hospital, Taipei, Taiwan;

²Graduate Institute of Clinical Medicine, College of Medicine, National Taiwan University, Taipei, Taiwan;

³Department of Otolaryngology, National Taiwan University Hospital and National Taiwan University College of Medicine, Taipei, Taiwan; ⁴Department of Pathology, National Taiwan University Hospital and National Taiwan University College of Medicine, Taipei, Taiwan; ⁵Department of Internal Medicine, National Taiwan University Hospital Hsin-Chu Branch, Hsinchu, Taiwan; ⁶Division of Allergy, Immunology and Rheumatology, Department of Internal Medicine, Shuang Ho Hospital, Taipei Medical University, New Taipei City, Taiwan;

⁷Department of Internal Medicine, National Taiwan University Hospital Yun-Lin Branch, Yun-Lin, Taiwan; ⁸Department of Otolaryngology, National Taiwan University Hospital Hsin-Chu Branch, Hsinchu, Taiwan;

⁹Department of Pathology, National Taiwan University Hospital Hsin-Chu Branch, Hsinchu, Taiwan; ¹⁰Department of Pathology, National Taiwan University Hospital Yun-Lin Branch, Yun-Lin, Taiwan;

¹¹Department of Otolaryngology, National Taiwan University Hospital, Taipei, Taiwan; ¹²Department of Nuclear Medicine, National Taiwan University Hospital and National Taiwan University College of Medicine, Taipei, Taiwan; ¹³Department of Ophthalmology, National Taiwan University Hospital, Taipei City, Taiwan;

¹⁴Department of Internal Medicine, National Taiwan University Cancer Center, Taipei, Taiwan.

Abstract Objective

Ultrasound-guided core needle biopsy (CNB) of major salivary glands is a less invasive alternative to minor salivary gland biopsy for diagnosing Sjögren's disease (SjD), reducing risks of neurological deficits and pain. However, the optimal CNB specimen length for adequate glandular surface area remains uncertain. This study aimed to determine and validate the optimal CNB specimen length thresholds.

Methods

This retrospective, dual-phase study included 119 consecutive patients undergoing submandibular gland CNB with an 18-gauge needle for suspicious chronic inflammatory sialadenitis. Specimen length, total surface area, and glandular surface area were recorded. A validation cohort (n=37) was analysed separately. Statistical analyses included correlation, regression, and ROC curve analysis.

Results

Specimen length correlated with glandular surface area ($\rho=0.69$, $p<0.001$). Multivariable analysis confirmed specimen length as a positive predictor ($p<0.001$) and fatty infiltration as a negative predictor ($p=0.003$) of glandular surface area. ROC analysis identified 7.6 mm as optimal for glandular surface area $\geq 4 \text{ mm}^2$, and 10.5 mm for $\geq 8 \text{ mm}^2$. Clinically significant haematomas occurred in 1.7% of cases. In the validation cohort, using the 7.6 mm threshold, PPV was 86.2%, and NPV 87.5% for glandular surface area $\geq 4 \text{ mm}^2$. For the 10.5 mm threshold, PPV was 76%, and NPV 100% for $\geq 8 \text{ mm}^2$.

Conclusion

A CNB specimen length of $\geq 7.6 \text{ mm}$ is sufficient for diagnosing SjD, while $\geq 10.5 \text{ mm}$ may be required for clinical trials. These findings may support the integration of specimen length thresholds into CNB procedural guidelines.

Key words

Sjögren's disease, ultrasound, echography, minimal invasiveness

Chiao-Feng Cheng, MD
 Tseng-Cheng Chen, MD, PhD*
 Min-Shu Hsieh, MD, PhD*
 Ting-Yuan Lan, MD
 Chung-Yen Huang, MD
 Jui-Hung Kao, MD
 Yu-Heng Lin, MD
 Chi Wang, MD
 Hsien-Neng Huang, MD
 Long-Wei Lin, MD
 Yu-Ju Chiang, MD
 Mei-Fang Cheng, MD, PhD
 Hsiao-Sang Chu, MD
 Yi-Min Huang, MD
 Cheng-Hsun Lu, MD, PhD
 Ko-Jen Li, MD, PhD
 Chieh-Yu Shen, MD, PhD
 Song-Chou Hsieh, MD, PhD

*Contributed equally.

Please address correspondence to:

Tseng-Cheng Chen
 no. 7, Zhongshan S. Road,
 Zhongzheng District,
 Taipei City 100, Taiwan (R.O.C.)
 E-mail: chenzengchang@ntuh.gov.tw

and to:

Min-Shu Hsieh
 (postal address as above)
 E-mail: hsiehmiangshu@ntuh.gov.tw

Received on July 26, 2025; accepted in
 revised form on November 17, 2025.

© Copyright CLINICAL AND
 EXPERIMENTAL RHEUMATOLOGY 2025.

*Funding: this work was supported by the
 National Science and Technology Council
 of Taiwan (grant no. 113-2314-B-002-318)
 and the National Taiwan University Hospital
 (grant no. 113-N0054 and 114-O0033).*

Competing interests: none declared.

Introduction

Salivary gland biopsy is crucial for diagnosing Sjögren's disease (SjD), as it enables the detection of focal lymphocytic sialadenitis, a histopathological hallmark of the disease (1). A focus score more than or equal to one in minor salivary glands has been incorporated into classification criteria for SjD (2-5). However, several drawbacks of minor salivary gland biopsy, including invasiveness, permanent sensory loss, and post-procedural pain (6-10), reduce its clinical utility, despite its relevance for disease severity assessment and prognosis (1, 11-14).

In contrast, major salivary gland biopsy remains underexplored for SjD diagnosis. Open parotid gland biopsy has demonstrated comparable diagnostic accuracy to minor salivary gland biopsy with modified histological criteria (15-18). Submandibular gland (SMG) biopsy may offer additional value for SMG's early involvement in SjD (19-21). Additionally, sialoscintigraphy parameters in SMG can differentiate SjD from non-specific sicca syndrome (22). These findings support the potential role of SMG biopsy in the early diagnosis of SjD. However, the invasiveness of open biopsy limits its routine use despite its diagnostic and prognostic potential (23, 24).

Ultrasound-guided core needle biopsy (CNB) has emerged as a minimally invasive alternative, offering short procedure times and low complication rates, and has shown promising results in diagnosing SjD (25-28). However, challenges remain. Fatty infiltration in the salivary glands, a common phenomenon in SjD (29-31), may affect identification of glandular surface area and compromise the specimen adequacy (27). While no specific guideline for diagnosing SjD using specimens from major salivary glands, most reports utilize the classical focus score, which requires a minimum glandular surface area of $\geq 4 \text{ mm}^2$ in clinical practice and $\geq 8 \text{ mm}^2$ for clinical trials (32). While specimen length may serve as a proxy for glandular surface area during the procedure, no consensus exists on the optimal CNB specimen length. This study aimed to define and validate

length-based adequacy thresholds for SMG CNB by identifying real-world predictors of glandular surface area.

Material and methods

Study design and participants

This study was conducted in two phases to determine the optimal specimen length required in ultrasound-guided CNB of the SMG for achieving adequate glandular surface area in the diagnosis of SjD. Ethical approval was obtained from the Institutional Review Board of our hospital (202307116RINA), and informed consent for this retrospective analysis was waived given its non-interventional design using existing clinical data and archived specimens.

Phase 1: Threshold identification (retrospective study)

In the first phase of this study, we retrospectively included all consecutive patients who underwent ultrasound-guided CNB of the SMG between July 2010 and January 2025 due to clinical suspicion of chronic or autoimmune salivary gland disease. The indications for SMG CNB included: (1) sicca symptoms with anti-SSA positivity when the patient declined a labial gland biopsy (with or without glandular swelling), (2) persistent submandibular gland swelling, or (3) diagnostic uncertainty in patients with chronic salivary gland symptoms. Only non-neoplastic biopsy specimens were included. In our centre and collaborating institutions, SMG CNB is routinely performed for non-neoplastic indications owing to its accessibility and established procedural familiarity. Although published data on SMG CNB remain limited, emerging studies have demonstrated its safety and diagnostic utility in inflammatory salivary gland diseases (25, 33).

Patients were classified into three groups based on final integrated diagnosis with clinical features, serology, imaging, histopathology, and treatment response: SjD (per ACR/EULAR 2016 criteria with anti-SSA) (3), IgG4RD (per 2019 criteria) (34), and chronic sialadenitis (non-autoimmune, histologically defined). A total of 119 cases were retrospectively enrolled in this phase.

Phase 2: Validation

(consecutive retrospective cohort)

To validate the study result in Phase 1, we conducted an independent validation study in the second phase using consecutively recruited SMG CNB specimens from one tertiary teaching hospital (National Taiwan University Hospital Hsin-Chu branch) and two regional hospitals (National Taiwan University Hospital Yun-Lin branch and National Taiwan University Cancer Centre) from July 2020 to January 2025. Only non-neoplastic biopsy specimens were included as well to align with the first phase's criteria. A total of 37 cases were retrospectively collected in phase 2.

Biopsy technique

Experienced otolaryngologists conducted a detailed assessment of the bilateral SMGs using a 12 MHz linear array transducer (Philips EPIQ5 diagnostic US system). The length of the SMG (anteroposterior length) was measured in the paramandibular plane to evaluate its potential impact on biopsy adequacy (35, 36). SMG biopsies were taken from the side with most ultrasonographic abnormalities. For the procedure, local anaesthesia with xylocaine 2% was administered. The ultrasound-guided CNB was performed using a free-hand technique with an 18-gauge needle (Temno Evolution™ Biopsy Devices, Cardinal Health Inc., Dublin, CA, USA) following local anaesthesia. The tissue fragments were stored in formalin immediately after sampling. Pressure was applied to the entry point of the needle for 15 minutes.

Histopathological evaluation

Tissue fragments were fixed in formalin, embedded in paraffin blocks, cut at a thickness of 4 µm, and stained with haematoxylin and eosin (H&E). All SMG biopsies were evaluated by an expert pathologist (M.H.H.) with specific head and neck pathology expertise, including SjD. H&E-stained sections were digitally scanned by a Hamamatsu NanoZoomer digital whole slide scanner. The total surface areas of the specimens, including adipose tissue, were identified, morphometrically compartmentalised on a 4x magnifi-

Table I. Basic characteristics of enrolled biopsy specimens.

Characteristics	Enrolled patients (n=119)
Male, n (%)	42 (35)
Age, year, median (IQR)	59 (17.5)
Length of SMG gland, mm, median (IQR)	30.5 (7.4) ^a
Pass of CNB sampling, median (IQR)	1 (1)
Specimen length, mm, median (IQR)	9.6 (4.7)
Total surface area, mm ² , median (IQR)	6.7 (4.9)
Glandular surface area, mm ² , median (IQR)	5.6 (5.8)
Fatty infiltration, %, median (IQR)	3.0 (9.1)
Diagnosis	
Sjögren's disease, n (%)	56 (47)
IgG4RD, n (%)	29 (24)
Chronic sialadenitis, n (%)	34 (29)
Clinically significant hematoma, n (%)	2 (1.7)

^aMissing data in one of the patients.

CNB: core needle biopsy; IgG4RD: IgG4 related disease; IQR: interquartile range; SMG: submandibular gland.

cation, and quantified on the surface (mm²). The length of the specimen was also measured. Given the frequent presence of extensive adipose replacement in SMG core needle biopsy specimens, and the technical limitation that most biopsy fragments are small and partially fragmented, we adopted a pragmatic approach: if any histologically identifiable glandular tissue (acini or ducts) was observed within a fragment, we considered the entire fragment as originating from glandular parenchyma, and its total surface area was included in the calculation of "glandular surface area." This approach was based on the procedural assurance that the needle was placed entirely within the submandibular gland under ultrasound guidance. In clinical practice, fragmented specimens with >80% adipose content are frequently encountered, yet still originate from the gland. We acknowledge that this method may overestimate the true proportion of preserved glandular parenchyma and address this limitation in the Discussion. The surface area of fatty infiltration was delineated manually by the 'Free Hand Region' function in the NDP.view (37), and recorded as the proportion of adipose tissue relative to the total surface area.

For specimens from patients with SjD, the H&E sections were further evaluated for the presence of lymphoepithelial lesions (LELs), ectopic germinal centres (GCs), and the maximal diameter of foci. The calculation of the focus score complied with previous rec-

ommendations (32, 38). Focus scores were calculated only for specimens with measurable glandular tissue. In line with prior recommendations emphasising the need for sufficient surface area to ensure focus score stability (32), we restricted focus score reporting to specimens with glandular surface area ≥4 mm². Specimens below this threshold were considered non-evaluable for focus score.

Statistical analysis

Demographic characteristics of patients are summarised with median with interquartile range (IQR) for continuous variables and numbers with percentages for categorical variables. Comparing the difference between the disease groups, Kruskal-Wallis test was used for continuous variables and Pearson's chi-squared test or Fisher's exact test were used for categorical variables by gtsummary package. Pearson correlation coefficients were calculated to assess the relationship between specimen length, total surface area of specimen, and glandular surface area. The receiver operating characteristic curves (ROC curves) and area under curves (AUCs) were conducted by cutpointr package. Positive predictive value (PPV) and negative predictive value (NPV) were also calculated. Univariable and multivariable analyses were calculated using linear regression to identify predictors of glandular surface area. For the multivariable analyses, the full model included all the candidate variables,

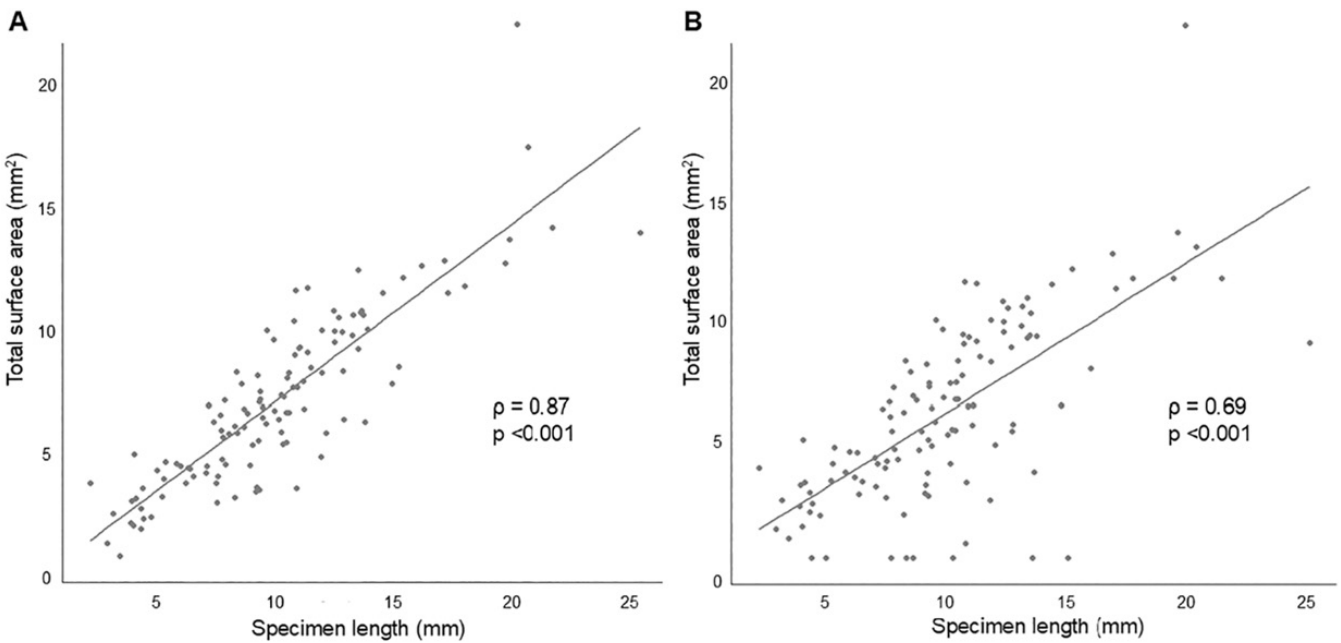


Fig. 1. Correlation between specimen length, total surface area, and glandular surface area. **A:** Correlation plot for specimen length and total surface area; **B:** Correlation plot for specimen length and glandular surface area.

Table II. Univariable and multivariable analysis for prediction of glandular surface area.

	Univariable analysis		Multivariable analysis (Full model)		Multivariable analysis (Reduced model)	
	β(95% CI)	p-value	β(95% CI)	p-value	β(95% CI)	p-value
Age	0.02 (-0.03–0.07)	0.460	0.01 (-0.03–0.05)	0.596	–	–
Male	0.76 (-0.68–2.20)	0.298	0.24 (-1.08–1.55)	0.720	–	–
Length of SMG gland	0.05 (-0.07–0.16)	0.420	0.00 (-0.08–0.09)	0.922	–	–
Specimen length	0.63 (0.51–0.75)	<0.001*	0.62 (0.50–0.74)	<0.001*	0.63 (0.51–0.75)	<0.001*
Diagnosis						
Chronic sialadenitis	Reference category	–	Reference category	–	Reference category	–
IgG4RD	1.36 (-0.53–3.26)	0.158	0.07 (-1.38–1.53)	0.919	0.25 (-1.10–1.59)	0.718
Sjögren’s disease	1.00 (-0.63–2.63)	0.226	1.63 (0.34–2.92)	0.014*	1.43 (0.25–2.62)	0.018*
Fatty infiltration	-0.05 (-0.10–0.00)	0.038*	-0.06 (-0.09 to -0.02)	0.003*	-0.05 (-0.09 to -0.02)	0.003*

*p<0.05
CI: confidence interval; IgG4RD: IgG4 related disease; SMG: submandibular gland.
The full model included all candidate variables. The reduced model retained only statistically significant variables (p<0.05) to improve interpretability while maintaining predictive accuracy. Full model results are provided for transparency.

while the reduced model retained only variables with $p<0.05$ to improve interpretability while maintaining predictive accuracy. A p -value <0.05 was considered statistically significant. All analyses were performed using R software version 4.4.1 (R Foundation for Statistical Computing, Vienna, Austria).

Results

Patients’ characteristics

A total of 119 receiving ultrasound-guided CNB of the SMG were enrolled in the first phase of the study. Fifty-six patients had SjD, 29 patients had IgG4RD, and 34 had chronic sialadenitis

(Table I). The length of SMGs, specimen length, total specimen surface, and glandular surface were not significantly different between the diseases (Supplementary Table S1), while the fatty infiltration is higher in patients with SjD. Among these specimens, 79 out of 119 presented with glandular surface area ≥ 4 mm². Two of the patients had clinically significant post-biopsy hematoma and were managed with conservative treatment without further intervention.

Correlation between specimen length and glandular surface area

The Pearson’s correlation showed that

the specimen length positively correlates with both total specimen surface ($\rho=0.87$, $p<0.001$) (Fig. 1A) and glandular surface ($\rho=0.69$, $p<0.001$) (Fig. 1B). These results support using specimen length as an approximate measure of the glandular surface area.

Specimen length may be an independent approximate for glandular surface area

Univariable and multivariable linear regression analyses were conducted to identify the predictors of glandular surface area (Table II). Multivariable analysis in full model revealed that

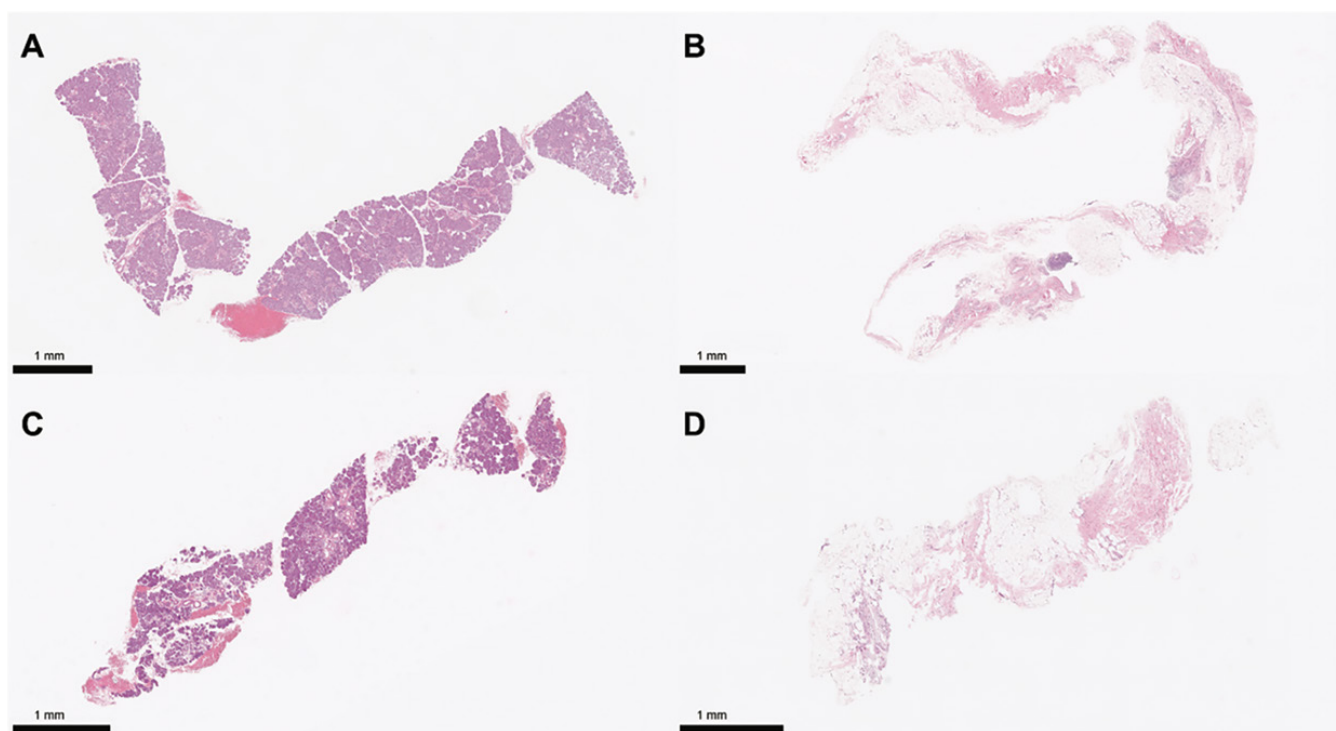


Fig. 2. Representative H&E-stained images of submandibular gland CNB specimens illustrating variations in fatty infiltration.

A: Long specimen with abundant glandular tissue, demonstrating high diagnostic value; **B:** Long specimen with high fatty infiltration; **C:** Short specimen with well-preserved glandular tissue; **D:** Short specimen with extensive fatty infiltration, highlighting how fat replacement can compromise biopsy adequacy.

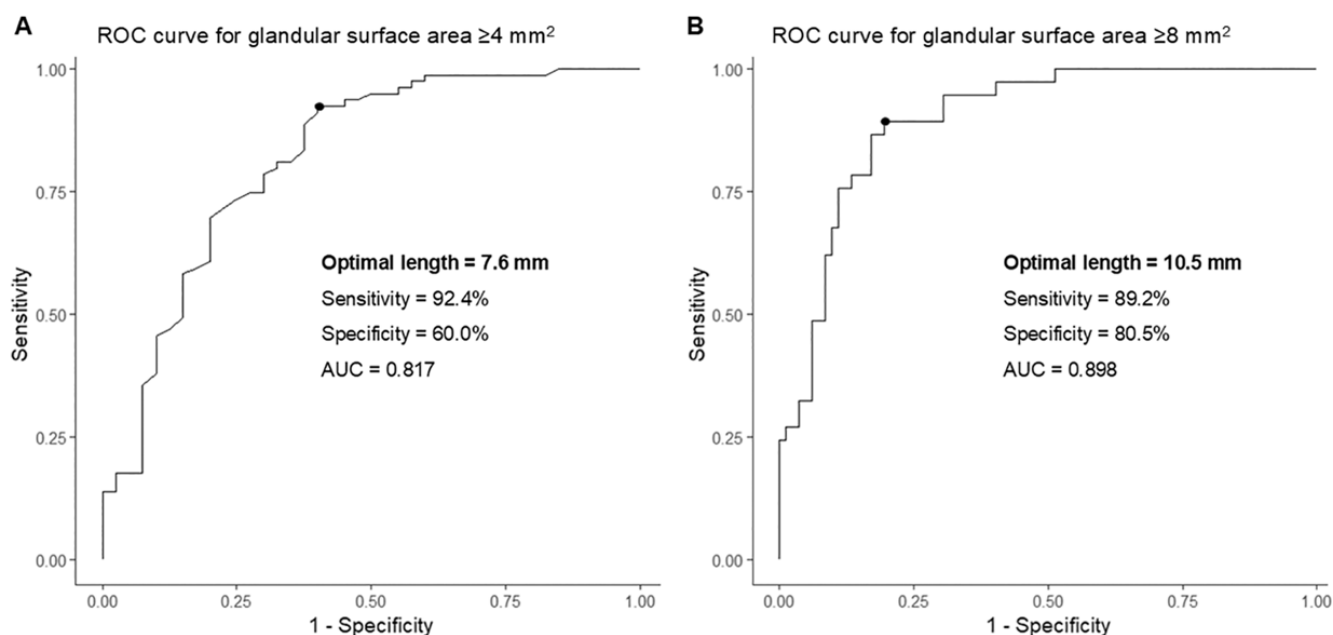


Fig. 3. ROC analysis for optimal specimen length for glandular area $\geq 4 \text{ mm}^2$ and $\geq 8 \text{ mm}^2$.

A: ROC curve for specimen length and glandular surface ($\geq 4 \text{ mm}^2$); **B:** ROC curve for specimen length and glandular surface ($\geq 8 \text{ mm}^2$).

specimen length remained the strongest independent predictor of glandular surface area ($\beta=0.62$, 95% CI: 0.50–0.74, $p<0.001$). Fatty infiltration was also significantly associated with lower glandular surface area ($\beta=-0.06$, 95% CI: -0.09 to -0.02, $p=0.003$), confirming

that adipose replacement compromises biopsy adequacy. In contrast, SMG size was not independently associated with glandular surface area ($\beta=0.00$, 95% CI: -0.08 to 0.09, $p=0.922$). Similarly, IgG4-related disease did not significantly influence biopsy ad-

equacy ($\beta=0.07$, 95% CI: -1.38 to 1.53, $p=0.919$). Notably, SjD was significant in the full model ($\beta=1.63$, 95% CI: 0.34–2.92, $p=0.014$) and remained significant in the reduced model ($\beta=1.43$, 95% CI: 0.25–2.62, $p=0.018$), suggesting that this disease independently af-

Table III. Predictive performance of specific specimen length for glandular surface area.

	First phase (threshold identification)		Second phase (validation cohort)	
	Specimen length ≥ 7.6 mm for glandular surface area ≥ 4 mm ²	Specimen length ≥ 10.5 mm for glandular surface area ≥ 8 mm ²	Specimen length ≥ 7.6 mm for glandular surface area ≥ 4 mm ²	Specimen length ≥ 10.5 mm for glandular surface area ≥ 8 mm ²
Length \geq threshold	88/119 (73.9%)	49/119 (41.2%)	29/37 (78.4%)	25/37 (67.6%)
Sensitivity	92.4%	89.2%	96.2%	100%
Specificity	60.0%	80.5%	63.6%	66.7%
PPV	82.0%	67.3%	86.2%	76.0%
NPV	80.0%	94.3%	87.5%	100%
AUC	0.817	0.898	0.799	0.833

AUC: area under curve; NPV: negative predictive value; PPV: positive predictive value.

fects glandular surface area adequacy when accounting for other variables. Table II presents the results from both the full and reduced models, with the reduced model retaining only variables with $p < 0.05$ to improve interpretability while maintaining predictive accuracy. The full model results are provided for transparency. To further illustrate the impact of fatty infiltration on biopsy adequacy, representative H&E-stained CNB specimens are shown in Figure 2. These images demonstrate that while longer specimens generally contain more glandular surface area, adipose infiltration can significantly reduce the diagnostic yield. Conversely, some shorter specimens may still provide adequate glandular content when composition is favourable.

Optimal specimen length to predict adequate glandular surface area

According to the above analyses, we plan to identify the optimal specimen length to obtain an adequate glandular surface area for clinical application. A glandular surface area of more than or equal to 4 mm² is the specimen adequacy criteria for diagnosing SjD (16, 27). In clinical trials, it has been proposed that a glandular surface area of more than or equal to 8 mm² should be obtained to select appropriate samples to be examined by focus score (33). We therefore conduct ROC analyses to determine the optimal specimen length for these two criteria for specimen adequacy of glandular surface area (Fig. 3A-B). The optimal specimen length for predicting glandular surface area ≥ 4 mm² is 7.6 mm, with sensitivity 92.4%, specificity 60.0%, and AUC 0.817. For glandular area ≥ 8 mm², the optimal

specimen length is 10.5 mm, with sensitivity 89.2%, specificity 80.5%, and AUC 0.898. Sensitivity analysis by serial exclusion of adipose-rich specimens (from 5% to 80%) demonstrated that discrimination by specimen length was robust across all lipid thresholds (Suppl. Tables S2 and S3, and Suppl. Fig. 1A-B). For the adequacy endpoint (glandular surface area ≥ 4 mm²), AUCs remained 0.811–0.837 and the optimal cut-point of 7.6 mm was unchanged despite exclusion up to 38.7% of cases (lipid $> 5\%$). For the trial-level endpoint (≥ 8 mm²), AUCs remained high (0.892–0.912) with a minimal shift of the optimal cut-point from 10.5 mm to 11.3 mm after excluding cases with lipid $> 10\%$.

Histological features in core needle biopsy specimens from patients with SjD

Among the 56 patients with SjD, 38 (67.9%) had CNB specimens with a glandular surface area ≥ 4 mm². Of these adequately sized specimens, 15 (39.5%) demonstrated a focus score ≥ 1 , and 18 (47.4%) showed either a focus score ≥ 1 or small lymphocytic infiltrates with LELs. Detailed histological characteristics are provided in Supplementary Table S4.

Validation for the thresholds of specimen length to predict the adequate glandular surface area

To validate the thresholds of specimen length for the glandular surface area, we retrospectively enrolled consecutive patients receiving SMGs by CNB from three other hospitals. A total of 37 patients were enrolled. When using specimen length ≥ 7.6 mm as the threshold, the sensitivity for glandular surface

area ≥ 4 mm² is 96.2%, and specificity is 63.6% with PPV 86.2% and NPV 87.5% (Table III). For specimen length ≥ 10.5 mm, the sensitivity for glandular surface area ≥ 8 mm² is 100%, and specificity is 66.7% with PPV 76.0%, and NPV 100%.

Interobserver reproducibility

To evaluate reproducibility of glandular tissue identification, an independent pathologist (C.Y.H.) re-evaluated all fragments following the same morphological criteria. Fragment-level agreement for the presence of glandular tissue was excellent (Cohen's $\kappa = 0.77$, $p < 0.001$). At the case level, agreement for biopsy adequacy was also high ($\kappa = 0.84$ for achieving ≥ 4 mm² of glandular area, and $\kappa = 1.00$ for ≥ 8 mm²). The glandular-to-total surface ratio, treated as a continuous variable, showed good reliability between observers (ICC(2,1) = 0.74, 95% CI 0.63–0.81, $p < 0.001$), supporting the robustness of the operational definition of glandular surface area and the reproducibility of adequacy classification.

Discussion

This study aims to address a procedural gap in current SjD diagnostics by establishing quantitative adequacy criteria for SMG CNB. We defined and validated length-based thresholds for SMG CNB adequacy in chronic inflammatory salivary gland diseases. The results demonstrate that a length of ≥ 7.6 mm is optimal for achieving a glandular surface area of > 4 mm², and ≥ 10.5 mm for a surface area of ≥ 8 mm², using an 18-gauge needle. In a validation cohort, these thresholds showed strong predictive performance (PPV 86.2% and NPV

87.5% for ≥ 4 mm²; PPV 76.0% and NPV 100% for ≥ 8 mm²). These findings provide a practical threshold for assessing real-time adequacy.

Salivary gland biopsy is the cornerstone for both diagnosis and mechanistic understanding of SjD. Labial gland biopsy remains the gold standard due to its accessibility and extensive validation within the latest ACR/EULAR classification criteria. Recent comparative studies have shown that major salivary gland specimens reveal complementary disease features, particularly enhanced B-cell-associated features in the parotid glands (39), and that ultrasound-guided CNB provides a minimally invasive approach. These findings suggest that major gland biopsies may complement labial biopsy in personalised SjD care.

Although the glandular surface area is essential for interpretation of labial gland specimen (40), the optimal glandular area in major salivary glands remains undetermined, especially in CNB. Deroo *et al.* reported that 14 of 20 parotid gland CNB specimens (18-gauge needle, two passes) achieved ≥ 4 mm², while Zabotti *et al.* achieved 100% adequacy using a 14-gauge needle (27, 28). These differences may reflect needle gauge and specimen size. To minimise procedural risks while ensuring tissue adequacy, we propose that specimen length can serve as a real-time intraoperative reference for guiding additional passes. While we used 4 mm² and 8 mm² as reference benchmarks based on established practice in labial gland biopsy, we acknowledge that the optimal glandular surface area for SMG diagnosis may differ due to anatomical and histological variations between glands. Our study offers a technical framework for consistently achieving these areas, although formal validation as diagnostic thresholds for SMG remains to be established.

Fatty infiltration in salivary glands is common in SjD and complicates histological interpretation (29, 30). As shown in Figure 2, even long specimens may be inadequate when dominated by fat, while shorter but preserved specimens may suffice. We pragmatically considered fragments containing any identifiable glandular tissue as glandu-

lar surface area, recognising that this approach may slightly overestimate functional parenchyma. However, sensitivity analyses indicated that this definition remained generally robust even in adipose- or fibrosis-rich specimens, with only a minor upward drift (0.8 mm) in the trial-grade threshold after excluding samples with $>10\%$ adipose tissue. Therefore, when pre-biopsy imaging reveals marked fat replacement, such as hyperechoic bands in ultrasound (41), operators may consider obtaining a slightly longer specimen (~ 11.3 mm to achieve an 8 mm² glandular surface area) or discussing alternative diagnostic approaches with patients.

In the histological evaluation, fatty infiltration also affects the interpretation of the focus score. Because focus score is calculated per 4 mm² of residual glandular area, extensive adipose or fibrotic replacement may artificially dilute the apparent density of lymphocytic foci. In such cases, the low focus score may reflect parenchymal destruction rather than the absence of the disease, particularly in long-standing SjD. Complementary histological features, such as LELs, GCs, and plasma cell shift, may therefore provide a more comprehensive assessment of glandular inflammation (42).

Whether histological criteria for major salivary gland CNB should be modified remains an open question. Evidence from parotid gland biopsy provides important context. Pijpe *et al.* showed that open parotid gland biopsy achieved diagnostic performance comparable to labial biopsy when LELs were incorporated with focus score ≥ 1 (16). This finding suggests that each salivary gland possesses unique histopathological characteristics that may require tailored diagnostic criteria.

In our cohort, only 39.5% of adequate SMG specimens reached focus score ≥ 1 , whereas 47.4% exhibited either focus score ≥ 1 or LELs, implying that including additional histological features could improve diagnostic sensitivity. Similarly, Zabotti *et al.* and Deroo *et al.* reported low focus score positivity in parotid CNB (27, 28). Nakshbandi *et al.* demonstrated $\sim 80\%$ labial-parotid concordance but stronger B-cell activa-

tion in parotid glands (higher GC density, more severe LELs) (39), while Van Ginkel *et al.* showed that incorporating multiple histopathological features beyond focus score alone increased diagnostic specificity from 88% to 100% in labial biopsies (42). Collectively, these findings support gland-specific adaptation of histological criteria, particularly for major gland CNB.

We hope that our study contributes to this evolving landscape by outlining technical parameters for SMG CNB. Labial gland biopsy remains the first-line and most validated diagnostic tool, whereas parotid gland biopsy serves as an alternative or second-line option in experienced centres and a valuable resource for studying B-cell-mediated pathology or lymphoma risk. The diagnostic and research roles of SMG biopsy are still being defined; preliminary data, including that from our cohort, suggest potential links to salivary function. Although both parotid and SMG CNB have demonstrated safety and feasibility under ultrasound guidance, SMG CNB may currently best be regarded as a third-line option, following labial (gold standard) and parotid (validated alternative) biopsies.

Biopsy site selection should be guided by diagnostic validation (strongest for labial), technical expertise, specific research aims (B-cell biology favours parotid), and patient factors. In this context, procedural adequacy, particularly in CNB, becomes critical for ensuring reliable interpretation. The length-based adequacy criteria established in this study (≥ 7.6 mm for diagnostic, ≥ 10.5 mm for research contexts) can be integrated into procedural checklists as intraoperative quality indicators to standardise sampling and reduce inadequate specimens. While current ACR/EULAR criteria do not yet include major salivary gland CNB, these results provide a bridge between procedural technique and diagnostic reliability, offering quantitative guidance for future consensus recommendations and biopsy-protocol updates. Until validated in multicentre studies, SMG CNB should be reserved for specific clinical situations where established biopsy methods are impractical or unavailable.

This study has several limitations. First, the study was conducted within a single institutional network in Taiwan, which may limit generalisability to other populations or procedural settings. Procedural techniques, such as the needle gauge, operator experience, and histopathologic patterns may vary across centres. Second, parotid glands were not included, and future studies should determine whether length thresholds differ for parotid CNB or other major glands. Third, because of the retrospective design, potential selection bias cannot be completely excluded despite the consecutive inclusion strategy and independent validation cohort. Fourth, our measurement approach may overestimate true glandular preservation. Fifth, our findings primarily apply to chronically inflamed or structurally altered SMGs, which constitute the usual indications for CNB in clinical practice. Further multicentre prospective studies are warranted to validate and extend these findings across different populations and salivary gland types.

Conclusion

A CNB specimen length of ≥ 7.6 mm using an 18-gauge needle is sufficient to achieve diagnostic adequacy for SjD, while ≥ 10.5 mm may be appropriate for research or trial settings. These findings may facilitate the incorporation of length-based thresholds into CNB protocols, providing a practical reference for clinicians. Our study lays the groundwork for future refinement of histological criteria and the integration of imaging-guided procedural strategies in major salivary gland biopsy for SjD.

References

- DANIELS TE, COX D, SHIBOSKI CH *et al.*: Associations between salivary gland histopathologic diagnoses and phenotypic features of Sjögren's syndrome among 1,726 registry participants. *Arthritis Rheum* 2011; 63(7): 2021-30. <https://doi.org/10.1002/art.30381>
- VITALI C, BOMBARDIERI S, JONSSON R *et al.*: Classification criteria for Sjögren's syndrome: a revised version of the European criteria proposed by the American-European Consensus Group. *Ann Rheum Dis* 2002; 61(6): 554-58. <https://doi.org/10.1136/ard.61.6.554>
- SHIBOSKI CH, SHIBOSKI SC, SEROR R *et al.*: 2016 American College of Rheumatology/European League Against Rheumatism Classification Criteria for Primary Sjögren's Syndrome: A Consensus and Data-Driven Methodology Involving Three International Patient Cohorts. *Arthritis Rheumatol* (Hoboken, NJ) 2017; 69(1): 35-45. <https://doi.org/10.1002/art.39859>
- SHIBOSKI SC, SHIBOSKI CH, CRISWELL L *et al.*: American College of Rheumatology classification criteria for Sjögren's syndrome: a data-driven, expert consensus approach in the Sjögren's International Collaborative Clinical Alliance cohort. *Arthritis Care Res* 2012; 64(4): 475-87. <https://doi.org/10.1002/acr.21591>
- DANIELS TE: Labial salivary gland biopsy in Sjögren's syndrome. Assessment as a diagnostic criterion in 362 suspected cases. *Arthritis Rheum* 1984; 27(2): 147-56. <https://doi.org/10.1002/art.1780270205>
- IKE RW, MCCOY SS: Bedside labial salivary gland biopsy (LSGBx: Lip biopsy): An update for rheumatologists. *Best Pract Res Clin Rheumatol* 2023; 37(1): 101839. <https://doi.org/10.1016/j.berh.2023.101839>
- VALDEZ RMA, MELO TS, SANTOS-SILVA AR, DUARTE A, GUEIROS LA: Adverse post-operative events of salivary gland biopsies: a systematic review and meta-analysis. *J Oral Pathol Med* 2022; 51(2): 152-59. <https://doi.org/10.1111/jop.13229>
- OLSSON P, EKBLAD F, HASSLER A *et al.*: Complications after minor salivary gland biopsy: a retrospective study of 630 patients from two Swedish centres. *Scand J Rheumatol* 2023; 52(2): 208-16. <https://doi.org/10.1080/03009742.2021.1999671>
- CAPORALI R, BONACCI E, EPIS O, BOBBIO-PALLAVICINI F, MORBINI P, MONTECUCCO C: Safety and usefulness of minor salivary gland biopsy: retrospective analysis of 502 procedures performed at a single center. *Arthritis Rheum* 2008; 59(5): 714-20. <https://doi.org/10.1002/art.23579>
- FRIEDMAN JA, MILLER EB, HUSZAR M: A simple technique for minor salivary gland biopsy appropriate for use by rheumatologists in an outpatient setting. *Clin Rheumatol* 2002; 21(4): 349-50. <https://doi.org/10.1007/s100670200094>
- TRIANAFYLLIAS K, BACH M, OTTO M, SCHWARTING A: Diagnostic value of labial minor salivary gland biopsy: histological findings of a large sicca cohort and clinical associations. *Diagnostics* 2023; 13(19). <https://doi.org/10.3390/diagnostics13193117>
- CHATZIS L, GOULES AV, PEZOULAS V *et al.*: A biomarker for lymphoma development in Sjögren's syndrome: salivary gland focus score. *J Autoimmun* 2021; 121: 102648. <https://doi.org/10.1016/j.jaut.2021.102648>
- RISSELADA AP, KRUIZE AA, GOLDSCHMEDING R, LAFEVER FP, BIJLSMA JW, VAN ROON JA: The prognostic value of routinely performed minor salivary gland assessments in primary Sjögren's syndrome. *Ann Rheum Dis* 2014; 73(8): 1537-40. <https://doi.org/10.1136/annrheumdis-2013-204634>
- KAKUGAWA T, SAKAMOTO N, ISHIMOTO H *et al.*: Lymphocytic focus score is positively related to airway and interstitial lung diseases in primary Sjögren's syndrome. *Respir Med* 2018; 137: 95-102. <https://doi.org/10.1016/j.rmed.2018.02.023>
- KROESE FGM, HAACKE EA, BOMBARDIERI M: The role of salivary gland histopathology in primary Sjögren's syndrome: promises and pitfalls. *Clin Exp Rheumatol* 2018; 36 (Suppl. 112): S222-33.
- PIJPE J, KALK WW, VAN DER WAL JE *et al.*: Parotid gland biopsy compared with labial biopsy in the diagnosis of patients with primary Sjögren's syndrome. *Rheumatology* 2007; 46(2): 335-41. <https://doi.org/10.1093/rheumatology/kei266>
- WISE CM, AGUDELO CA, SEMBLE EL, STUMPTTE, WOODRUFF RD: Comparison of parotid and minor salivary gland biopsy specimens in the diagnosis of Sjögren's syndrome. *Arthritis Rheum* 1988; 31(5): 662-66. <https://doi.org/10.1002/art.1780310512>
- MARX RE, HARTMAN KS, RETHMAN KV: A prospective study comparing incisional labial to incisional parotid biopsies in the detection and confirmation of sarcoidosis, Sjögren's disease, sialosis and lymphoma. *J Rheumatol* 1988; 15(4): 621-29.
- VINAGRE F, SANTOS MJ, PRATA A, DA SILVA JC, SANTOS AI: Assessment of salivary gland function in Sjögren's syndrome: the role of salivary gland scintigraphy. *Autoimmun Rev* 2009; 8(8): 672-76. <https://doi.org/10.1016/j.autrev.2009.02.027>
- JENSEN SB, VISSINK A: Salivary gland dysfunction and xerostomia in Sjögren's syndrome. *Oral Maxillofac Surg Clin North Am* 2014; 26(1): 35-53. <https://doi.org/10.1016/j.coms.2013.09.003>
- PIJPE J, KALK WW, BOOTSMAN H, SPIJKERVET FK, KALLEMBERG CG, VISSINK A: Progression of salivary gland dysfunction in patients with Sjögren's syndrome. *Ann Rheum Dis* 2007; 66(1): 107-12. <https://doi.org/10.1136/ard.2006.052647>
- GARCÍA-GONZÁLEZ M, GONZÁLEZ-SOTO MJ, GÓMEZ RODRÍGUEZ-BETHENCOURT M, FERRAZ-AMARO I: The validity of salivary gland scintigraphy in Sjögren's syndrome diagnosis: comparison of visual and excretion fraction analyses. *Clin Rheumatol* 2021; 40(5): 1923-31. <https://doi.org/10.1007/s10067-020-05462-0>
- DELLI K, HAACKE EA, KROESE FG *et al.*: Towards personalised treatment in primary Sjögren's syndrome: baseline parotid histopathology predicts responsiveness to rituximab treatment. *Ann Rheum Dis* 2016; 75(11): 1933-38. <https://doi.org/10.1136/annrheumdis-2015-208304>
- HAACKE EA, VAN DER VEGT B, MEINERS PM *et al.*: Abatacept treatment of patients with primary Sjögren's syndrome results in a decrease of germinal centres in salivary gland tissue. *Clin Exp Rheumatol* 2017; 35(2): 317-20.
- GIOVANNINI I, LORENZON M, MANFRÈ V *et al.*: Safety, patient acceptance and diagnostic accuracy of ultrasound core needle biopsy of parotid or submandibular glands in primary Sjögren's syndrome with suspected salivary gland lymphoma. *RMD Open* 2022; 8(1). <https://doi.org/10.1136/rmdopen-2021-001901>
- BAER AN, GRADER-BECK T, ANTIOCHOS B, BIRNBAUM J, FRADIN JM: Ultrasound-

- guided biopsy of suspected salivary gland lymphoma in Sjögren's syndrome. *Arthritis Care Res* 2021; 73(6): 849-55. <https://doi.org/10.1002/acr.24203>
27. DEROO L, GENBRUGGE E, DOCHY F *et al.*: Ultrasound-guided core needle biopsy and incisional biopsy of the parotid gland are comparable in diagnosis of primary Sjögren's syndrome. *Rheumatology* 2023; 62(8): 2765-72. <https://doi.org/10.1093/rheumatology/keac714>
 28. ZABOTTI A, PEGOLO E, GIOVANNINI I *et al.*: Usefulness of ultrasound guided core needle biopsy of the parotid gland for the diagnosis of primary Sjögren's syndrome. *Clin Exp Rheumatol* 2022; 40(12): 2381-86. <https://doi.org/10.55563/clinexprheumatol/5n49yj>
 29. IZUMI M, EGUCHI K, NAKAMURA H, NAGATAKI S, NAKAMURA T: Premature fat deposition in the salivary glands associated with Sjögren syndrome: MR and CT evidence. *AJNR Am J Neuroradiol* 1997; 18(5): 951-58.
 30. SKARSTEIN K, AQRAWI LA, ØJORDSBAKKEN G, JONSSON R, JENSEN JL: Adipose tissue is prominent in salivary glands of Sjögren's syndrome patients and appears to influence the microenvironment in these organs. *Autoimmunity* 2016; 49(5): 338-46. <https://doi.org/10.1080/08916934.2016.1183656>
 31. LEEHAN KM, PEZANT NP, RASMUSSEN A *et al.*: Fatty infiltration of the minor salivary glands is a selective feature of aging but not Sjögren's syndrome. *Autoimmunity* 2017; 50(8): 451-57. <https://doi.org/10.1080/08916934.2017.1385776>
 32. FISHER BA, JONSSON R, DANIELS T *et al.*: Standardisation of labial salivary gland histopathology in clinical trials in primary Sjögren's syndrome. *Ann Rheum Dis* 2017; 76(7): 1161-68. <https://doi.org/10.1136/annrheumdis-2016-210448>
 33. LI ZZ, ZHU H, LI W, GAO Y, SU JZ, YU GY: Utility of navigation system-guided submandibular gland core needle biopsy in the diagnosis of immunoglobulin G4-related sialadenitis. *Int J Oral Maxillofac Surg* 2023; 52(9): 1005-12. <https://doi.org/10.1016/j.ijom.2023.01.007>
 34. WALLACE ZS, NADEN RP, CHARI S *et al.*: The 2019 American College of Rheumatology/European League Against Rheumatism classification criteria for IgG4-related disease. *Arthritis Rheumatol* 2020; 72(1): 7-19. <https://doi.org/10.1002/art.41120>
 35. ONKAR D, ONKAR P: Submandibular gland biometry by high frequency ultrasound. *J Anatom Soc India* 2016; 65(2): 156-58. <https://doi.org/10.1016/j.jasi.2017.01.006>
 36. DOST P, KAISER S: Ultrasonographic biometry in salivary glands. *Ultrasound Med Biol* 1997; 23(9): 1299-303. [https://doi.org/10.1016/s0301-5629\(97\)00152-x](https://doi.org/10.1016/s0301-5629(97)00152-x)
 37. Hamamatsu.com. NDP.view2 U12388-01.
 38. GREENSPAN JS, DANIELS TE, TALAL N, SYLVESTER RA: The histopathology of Sjögren's syndrome in labial salivary gland biopsies. *Oral Surg Oral Med Oral Pathol* 1974; 37(2): 217-29. [https://doi.org/10.1016/0030-4220\(74\)90417-4](https://doi.org/10.1016/0030-4220(74)90417-4)
 39. NAKSHBANDI U, VAN GINKEL MS, VERSTAPPEN G *et al.*: Histopathological comparison of Sjögren-related features between paired labial and parotid salivary gland biopsies of sicca patients. *Rheumatology* 2024; 63(10): 2670-77. <https://doi.org/10.1093/rheumatology/keae154>
 40. TRYPOSKIADIS K, NAYAR S, PUCINO V *et al.*: Increasing the number of minor salivary glands from patients with Sjögren's disease improves the diagnostic and measurement precision of the histological focus score. *Ann Rheum Dis* 2025; 84(4): 601-8. <https://doi.org/10.1016/j.ard.2025.01.038>
 41. TAKAGI Y, SASAKI M, EIDA S *et al.*: Comparison of salivary gland MRI and ultrasonography findings among patients with Sjögren's syndrome over a wide age range. *Rheumatology* 2022; 61(5): 1986-96. <https://doi.org/10.1093/rheumatology/keab560>
 42. VAN GINKEL MS, NAKSHBANDI U, ARENDS S *et al.*: Increased diagnostic accuracy of the labial gland biopsy in primary Sjögren syndrome when multiple histopathological features are included. *Arthritis Rheumatol* 2024; 76(3): 421-28. <https://doi.org/10.1002/art.42723>